INFECTION AND IMMUNITY, May 2000, p. 2655–2662 Vol. 68, No. 5
0019-9567/00/$04.00+0

Pathogenic Mycobacteria Disrupt the Macrophage Actin Filament Network

ISABELLE GUÉRIN AND CHANTAL DE CHASTELLIER*

INSERM U411, UFR de Médecine Necker, 75730 Paris Cedex 15, France

Received 28 December 1999/Returned for modification 3 February 2000/Accepted 17 February 2000

Phagosomes with pathogenic mycobacteria retain fusion and intermingling characteristics of early endosomes indefinitely. The time course of acquisition of newly endocytosed tracers becomes, however, atypical (lag instead of immediate acquisition) starting from day 1 postinfection (p.i.), thereby suggesting that additional factors affect this process. Disruption of the actin filament (F-actin) network by cytochalasin D perturbs the movement of early endosomes and probably fusion events among early endosomes and phagosomes. Here we compare, by immunofluorescence microscopy, the morphology and distribution of F-actin in macrophages infected with virulent *Mycobacterium avium*, in uninfected macrophages, or in macrophages after phagocytosis of nonpathogenic bacteria (*Mycobacterium smegmatis* or *Bacillus subtilis*) or hydrophobic latex particles. In uninfected cells, F-actin appeared as a network of small filaments distributed throughout the cell; about 80% of the cells also displayed one or two small patches of F-actin at the cell periphery. Virulent *M. avium* caused a marked disorganization of the F-actin network starting from day 1 p.i. The most salient features were the formation of several large patches, the progressive disappearance of the small filaments, and the appearance of large numbers of tiny punctate structures starting from day 2 p.i. With the three other particles, the F-actin network was unmodified compared to that in uninfected cells. The atypical lag in acquisition of newly endocytosed tracers by *M. avium*-containing phagosomes, therefore, seems to coincide with the disorganization of the F-actin network.

After phagocytic uptake of nonpathogenic microorganisms, the newly formed phagosomes become part of the organelles of the endocytic pathway and participate normally in its events and mechanisms (reviewed in references 1, 3, and 8). They immediately intermingle contents and membrane with early endosomes and undergo gradual modifications by specific addition and removal of membrane constituents (12, 14). This results in a process of maturation of the newly formed phagosomes. One of the important functional characteristics of the maturation process is that newly formed phagosomes, like early endosomes, mature to a state where they no longer fuse with early (or maturing) endosomes; only then can they fuse with lysosomes (reviewed in reference 8). This ultimately leads to killing and degradation of nonpathogenic microorganisms within the potent cytolytic environment of the acidic, hydrolase-rich phagolysosomes.

Phagosomes with pathogenic mycobacteria fuse with early endosomes (6, 11, 34, 37), but they are unable to mature. Accordingly, they do not fuse with lysosomes (2, 7, 10, 11, 18). Being immature, early-endosome-like, *Mycobacterium avium*-containing phagosomes should acquire newly internalized content marker immediately (9, 36, 40). This was indeed the case when the marker horseradish peroxidase (HRP) was added to cells within the first 3 h following infection (C. Fréhel, I. Guérin, and C. de Chastellier, unpublished observations). However, when HRP was added at later time points, i.e., between days 1 and 15 postinfection, it appeared at detectable levels in phagosomes only 10 to 20 min after uptake (11). This atypical time course of acquisition of HRP for a phagosome with early endosome characteristics suggested that additional factors were involved in this process.

* Corresponding author. Mailing address: INSERM U411, UFR de Médecine Necker, 156 rue de Vaugirard, 75730 Paris Cedex 15, France. Phone: 33 1 40 61 53 78. Fax: 33 1 40 61 55 92. E-mail: dechaste@citi2.fr.

Phagosome processing is a complex phenomenon that involves many cellular constituents including the cytoskeletal elements, i.e., microtubules and the actin filament network (reviewed in reference 3). Microtubules interact directly with endocytic compartments. They are required for organelle movement and for maintenance of late endocytic organelles in the juxtanuclear region (reviewed in references 4, 5, and 38), and they facilitate delivery of ligands to the degradative compartments (16). They interact with phagosomes in a similar manner (reviewed in references 4 and 5).

Several studies have shown that actin filaments are involved in endocytosis (21, 26, 27; reviewed in reference 33). They increase the uptake of ligands and their delivery to the degradative compartments (16, 39) downstream of the region where microtubules are required (16). Recent evidence also argues for a role of the actin filaments in the motility and distribution of early endosomes via Rho protein Rho D (29). Concerning phagocytosis, it is well established that the actin cytoskeleton is important for the earliest steps (24; reviewed in references 22, 23, and 35). Entry of a particle into a cell by phagocytosis indeed requires reorganization of the actin-based cytoskeleton underlying the region of the plasma membrane that contacts the particle. It is, however, not known to what extent the actin filament network is required for interaction of phagosomes with early and/or late organelles of the endocytic pathway. The fact that actin-binding proteins have been found in association with phagosomes containing latex particles (13) suggests that this could be the case.

Based on the above studies, and also because several pathogens have developed strategies to use the actin cytoskeleton to their own advantage (reviewed in references 15 and 25), we undertook the present study to examine whether pathogenic mycobacteria were able to alter the actin filament network. Our hypothesis was that, in doing so, they would perturb the movement of early endosomes, as is the case after treatment with cytochalasin D (29). This could explain, at least in part,

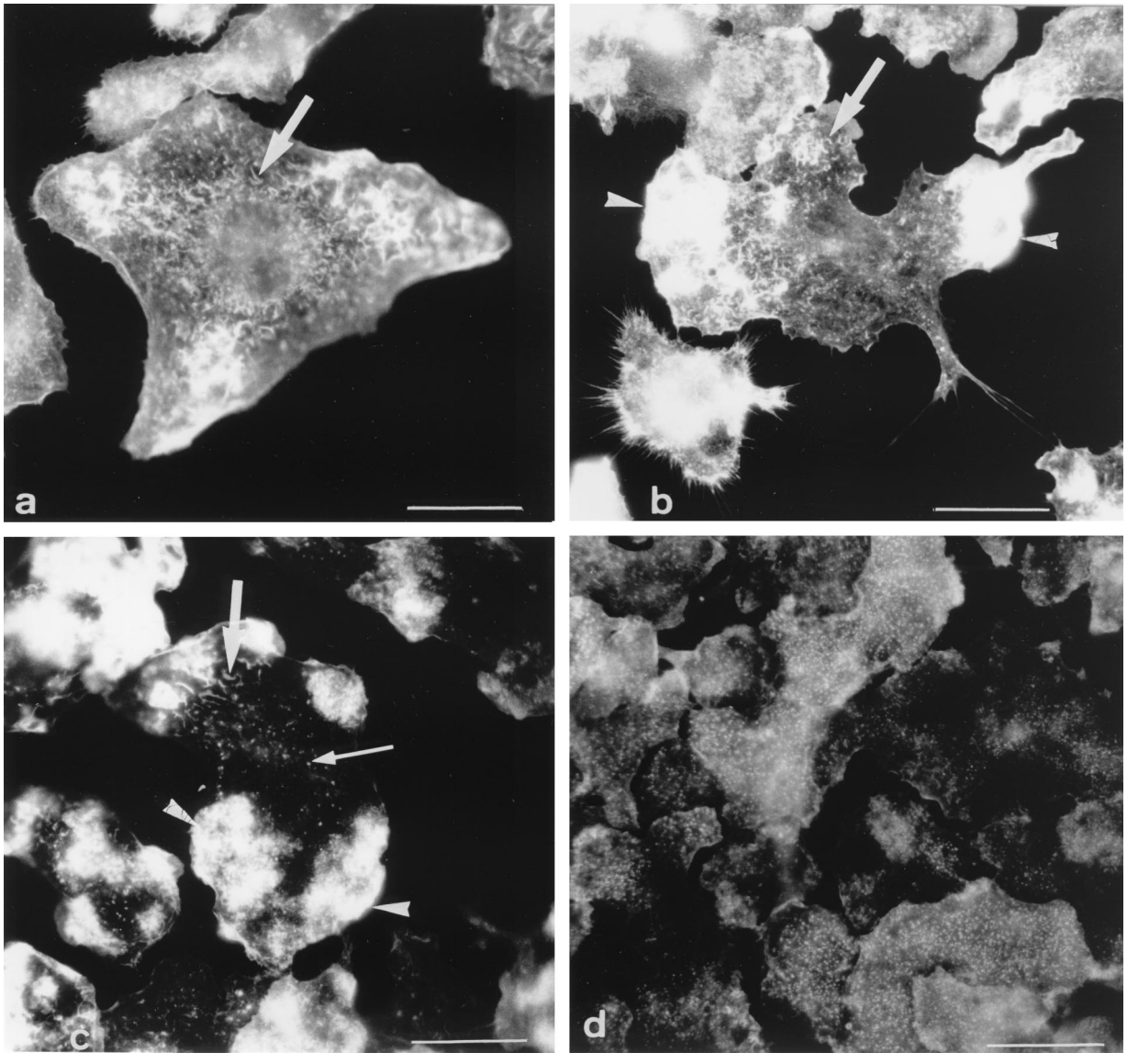

FIG. 1. General view of the four categories of cells as defined in terms of the morphological appearance and distribution pattern of the F-actin network after staining with fluorescent β-phalloidin. (a) Category 1: small filaments (arrow) and no patches; (b) category 2: small filaments (arrow) and one or two patches (arrowhead); (c) category 3: three to six large patches (arrowheads), a decrease in the number of small filaments (large arrow), and the appearance of punctate structures (small arrow); (d) category 4: abundant punctate structures, no filaments, and fragmented patches or no patches, as here. Bars = 5 μm.

the delayed and/or limited fusion with early endosomes observed before (11).

To test this possibility, bone marrow-derived (BMD) mouse macrophages (Mφs) were infected with a virulent strain of *M. avium* (19) used in previous work (11, 20). At selected time points after infection, the morphological appearance and distribution pattern of the actin filament network were examined by conventional immunofluorescence microscopy and compared to those of uninfected cells. As a control, the same study was undertaken after phagocytic uptake of the nonpathogenic mycobacterium *Mycobacterium smegmatis*, the nonpathogenic, rapidly degraded bacterium *Bacillus subtilis*, or inert hydrophobic latex particles.

MATERIALS AND METHODS

Phagocytic particles. (i) *M. avium*. *M. avium* TMC 724 (serovar 2) was cultured as described before (20). Because *M. avium* tends to lose its virulence in culture, we expanded bacteria of a first passage after isolation from mouse spleen and liver of C57BL/6 mice infected 6 to 8 weeks previously. Only bacteria of this first passage, grown on Middlebrook 7H10 agar plates (Difco Laboratories, Detroit, Mich.) supplemented with 0.05% Tween 80, 0.2% glycerol, and 10% oleic acid-albumin-dextrose-catalase (OADC) (Difco Laboratories), were used for experiments. Under these conditions, all colonies were smooth and transparent and more than 95% of the bacteria were morphologically intact and viable. Aliquots of bacterial suspensions were stored at −80°C. When required, frozen samples were quickly thawed, vortexed, and adjusted to the desired titer in Mφ culture medium.

(ii) *M. smegmatis*. *M. smegmatis* pJC86 (32) was cultured for 24 h at 37°C, without agitation, in Middlebrook 7H9 liquid medium supplemented with 0.05% Tween 80, 0.2% glycerol, 10% OADC (Difco Laboratories), and 30 μg of kanamycin per ml. Aliquots of concentrated bacterial suspension were stored at −80°C. When required, frozen samples were quickly thawed, vortexed, and adjusted to the desired titer in complete cell culture medium.

(iii) *B. subtilis*. *B. subtilis* strain MO 719 was cultured as described before (11) and used immediately for phagocytic uptake. More than 95% of the bacilli were morphologically intact and viable.

(iv) Fluoresbrite YG microspheres. These microspheres (i.e., fluorescein-labeled hydrophobic polystyrene beads; Polysciences/Fischer Scientific, Elancourt,

France) are 1 μm in diameter. The original bead solution, which was a suspension of 2.5% aqueous solids, was diluted 150-fold in complete Mϕ culture medium and used immediately for phagocytosis experiments.

Cell culturing and phagocytic uptake. BMD Mϕs were obtained by seeding bone marrow cells from 6- to 8-week-old C57BL/6 female mice in tissue culture dishes (ATGC Biotechnologie, Noisy-le-Grand, France) containing sterile glass coverslips. Cells were cultured as described before (11, 20). Particles were added to 7-day-old Mϕ cultures as follows.

(i) *M. avium.* Cells were incubated for 4 h at a bacterium-to-Mϕ ratio of 20:1, washed in four rinses of ice-cold phosphate-buffered saline (PBS) to eliminate noningested bacteria, and refed with fresh medium devoid of antibiotics. The medium was renewed three times a week.

(ii) *M. smegmatis.* Cells were incubated for 2 h at a bacterium-to-Mϕ ratio of 5:1, washed with PBS as described above, and refed with fresh medium. Because residual bacteria are able to multiply within the Mϕ culture medium, infected cells were washed and refed with fresh medium once a day.

(iii) *B. subtilis.* Cells were incubated at a bacterium-to-Mϕ ratio of 50:1 for 5 min or 10:1 for 45 min. In the latter case, cells were either fixed immediately or washed with PBS as described above and reincubated for up to 2 h in bacterium-free medium before being fixed.

(iv) Fluoresbrite microspheres. Cells were given latex beads for 30 min, washed with PBS as described above, and reincubated for 0 to 2 h in latex-free medium.

Immunofluorescence microscopy. All steps, including fixation of samples, were carried out at room temperature. At selected intervals before, during, or after phagocytic uptake of the various particles, cells grown on coverslips were fixed for 30 min with 3% paraformaldehyde (Sigma Chemical Co., St. Louis, Mo.) in PBS and washed in several rinses of PBS. Cells were either processed immediately for labeling of F-actin and immunodetection of bacteria within phagosomes or stored at 4°C for up to 4 days before being processed as follows. Cells were quenched with 50 mM NH_4Cl in PBS, permeabilized for 1 min with 0.5% Triton X-100 in PBS, washed with 0.2% gelatin-containing PBS (PBS-G), preincubated for 30 min with 5% normal goat serum in PBS to mask nonspecific sites at the surfaces of Mϕs, and washed with PBS-G. For immunodetection of *M. avium*, cells were first incubated for 30 min with the monoclonal antibody CS-17, immunoglobulin (Ig) isotype IgG3, raised against cell wall glycopeptidolipids extracted from mycobacteria of the same serovar as the strain used in the present work. The antibodies were diluted 8,000-fold prior to use. Cells were then incubated for 30 min with Alexa 488 (green)-conjugated goat anti-mouse IgG antibodies (Molecular Probes, Eugene, Oreg.) diluted 100-fold. For immunodetection of *B. subtilis*, cells were incubated with affinity-purified rabbit anti-*B. subtilis* antibodies directly conjugated to fluorescein isothiocyanate. For immunodetection of *M. smegmatis*, we had no specific antibodies. Bacterial DNA was therefore stained for 30 min with ethidium bromide (red) (Eurobio, Les Ulis, France) diluted 4,000-fold. To stain F-actin, cells were incubated for 30 min with fluorescent β-phalloidin conjugated to Alexa 568 (red) at 1.5 U per ml (β-phalloidin conjugated to Alexa 488 [green] was used instead when ethidium bromide was used to label *M. smegmatis*). All antibodies and reagents used for labelings were diluted in PBS-G, and each incubation step was followed by three washes with PBS-G. After the labeling steps, coverslips were washed twice with distilled water and mounted in Moviol (Sigma). Cells were examined immediately or stored at −20°C prior to observation. Cells were viewed with a Leitz DMRB microscope (Leica, Rueil Malmaison, France).

RESULTS AND DISCUSSION

Morphological appearance of the F-actin network. The F-actin network was examined after staining of fixed cells with β-phalloidin. When used under the conditions described above, this widely used drug binds only to F-actin. Observation of a large number of Mϕs and under a variety of experimental conditions led us to define four major types of cells in terms of the morphological appearance and distribution pattern of the F-actin network. These four categories, shown in Fig. 1, can be described as follows. (i) Cells of category 1 displayed short and thin filaments distributed throughout the cell (Fig. 1a) and no patches of F-actin. (ii) Mϕs of category 2 displayed short filaments identical to those observed in cells of category 1 (Fig. 1b). In addition, they contained one or two patches of F-actin (Fig. 1b). (iii) Cells of category 3 were characterized by the presence of three to six large patches of F-actin (Fig. 1c). The filaments were less abundant and were smaller than those of category 1 and 2 cells. (iv) In cells of category 4, the filaments completely disappeared and F-actin had a very characteristic punctate appearance (Fig. 1d). These cells either displayed several small patches (not shown) or no patches of F-actin (Fig. 1d). The percentage of cells of each category was determined in uninfected Mϕs and after phagocytic uptake of live pathogenic *M. avium* and other nonpathogenic bacteria or inert particles.

TABLE 1. Percentages of cells of the four different categories at selected time points after phagocytic uptake of particles[a]

Phagocytic particle	Time after uptake[b]	% Cells of category[c]:			
		1	2	3	4
None	NA[d]	18	82	0	0
B. subtilis	45 min	20	80	0	0
Latex beads	2 h	18	82	0	0
M. smegmatis	1 day	23	77	0	0
M. avium	2 h	24	76	0	0
	1 day	0	21	79	0
	2 days	0	2	38	60
	6 days	0	0	0	100

[a] For each particle and time point, counts were made on Mϕs in triplicate monolayers. Each value represents the mean of three determinations on 200 cells each. The standard error of the mean was between 5 and 10%. Data are from a typical experiment.
[b] Uninfected cells were cultured in parallel to *M. avium*-infected ones, and counts were done at the same time points for both cases. The data were taken on day 6. Identical results were obtained at all other time points.
[c] Categories were defined according to the morphological state and distribution of actin filaments (Fig. 1).
[d] NA, not applicable.

Appearance of the actin filament network in uninfected cells. Although F-actin is subjected to frequent assembly-and-disassembly events that lead to changes of shape and distribution of the F-actin network during endocytosis and cell movement, uninfected BMD Mϕs displayed a very reproducible morphology and distribution pattern of F-actin. The most salient feature was the presence of a network of short and thin filaments distributed throughout the cell (Fig. 1a and b). As indicated in Table 1, about 80% of the cells also displayed one or two patches of F-actin at the cell periphery (Fig. 1b); the remainder showed no patches (Fig. 1a). The two other categories, depicted in Fig. 1c and d, were never encountered in uninfected cells. Finally, as in many cell types, F-actin underlay the plasma membrane and filled the filopodia. Unlike other cell types, these Mϕs did not display actin cables. Cells were maintained in culture for up to 21 days. During this entire period, the F-actin network retained the same features as those described above. This characteristic appearance served as a basis for examining eventual modifications brought about by the presence of pathogenic mycobacteria.

Live pathogenic mycobacteria profoundly modify the actin filament network. Seven-day-old BMD Mϕs were infected with *M. avium* TMC 724. We adopted culture conditions such that this strain yields only transparent colonies. These bacteria are virulent for mice, as they proliferate within the reticuloendothelial organs of mice susceptible to mycobacterial infections (reviewed in reference 31), such as the C57BL/6 mice (19) used here, and ultimately cause death of such mice within 2 to 3 months after intravenous infection with 10^7 to 2×10^7 bacteria (C. Fréhel, and C. de Chastellier, unpublished observations). They also multiply within BMD Mϕs from the same mice with a generation time of 36 to 40 h (10, 20).

At selected time points after infection (0, 1, 2, 4, 6, and 10 days), cells were fixed and F-actin was stained with β-phalloidin (Fig. 2a to c). Phagosomes were visualized in the same cells by labeling bacteria with specific antibodies (Fig. 2d to f). Infected Mϕs were systematically labeled first for immunodetection of bacteria and then for F-actin; the converse proce-

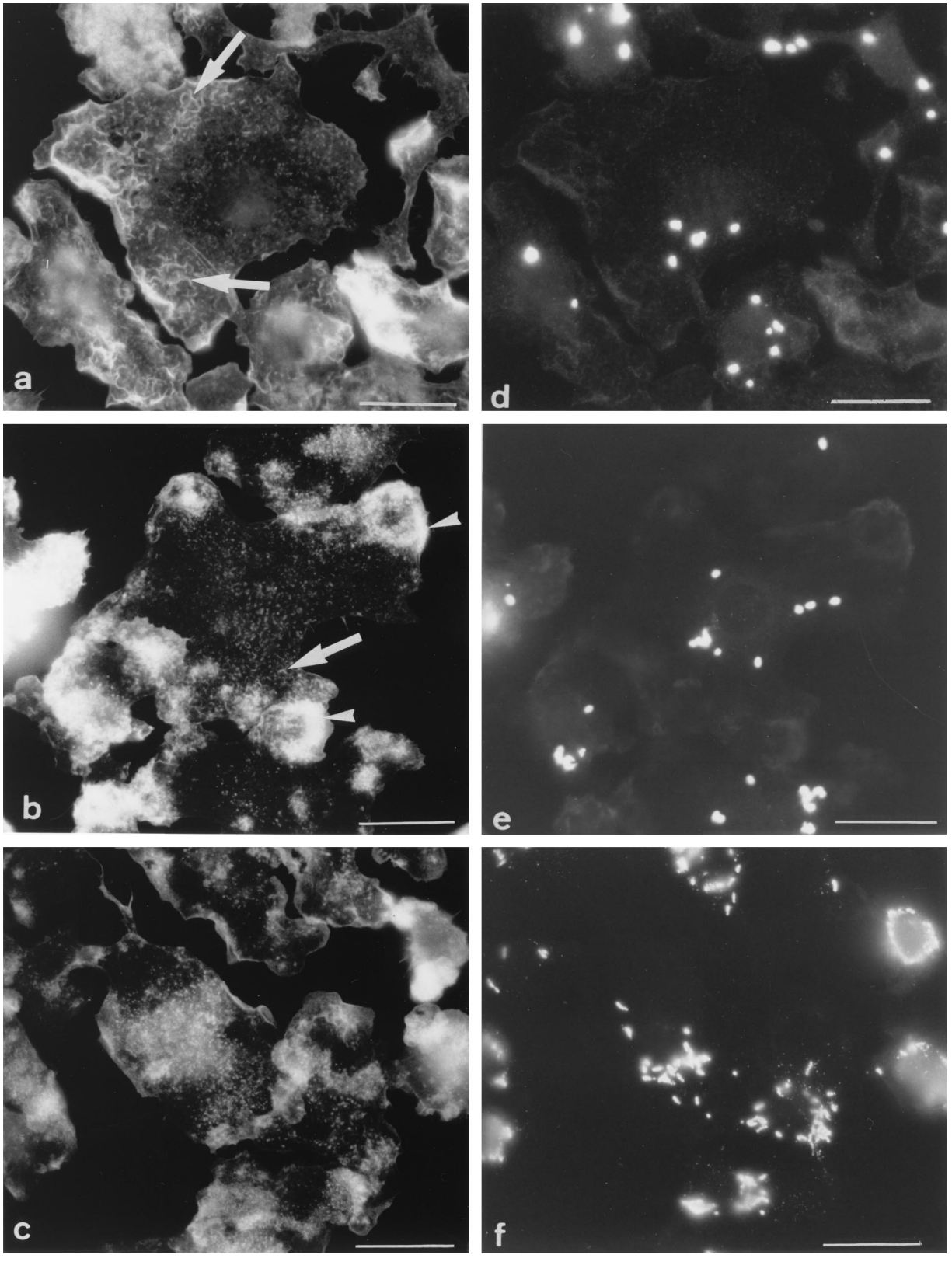

FIG. 2. Appearance of F-actin in Mϕs infected with *M. avium*. Cells were double labeled for F-actin (a to c) and for immunodetection of bacteria (d to f) at 0 (a and d), 1 (b and e), or 6 (c and f) days after a 4-h infection with *M. avium*. (a) Day 0: same F-actin pattern as in uninfected cells, i.e., abundance of small filaments (arrows); (b) day 1: accumulation of F-actin in several large patches (arrowhead); (c) day 6: F-actin showing a punctate appearance. In the same cells, phagosomes were scattered at days 0 (d) and 1 (e) and were gathered around the nucleus at day 6 (f). Bars = 5 μm.

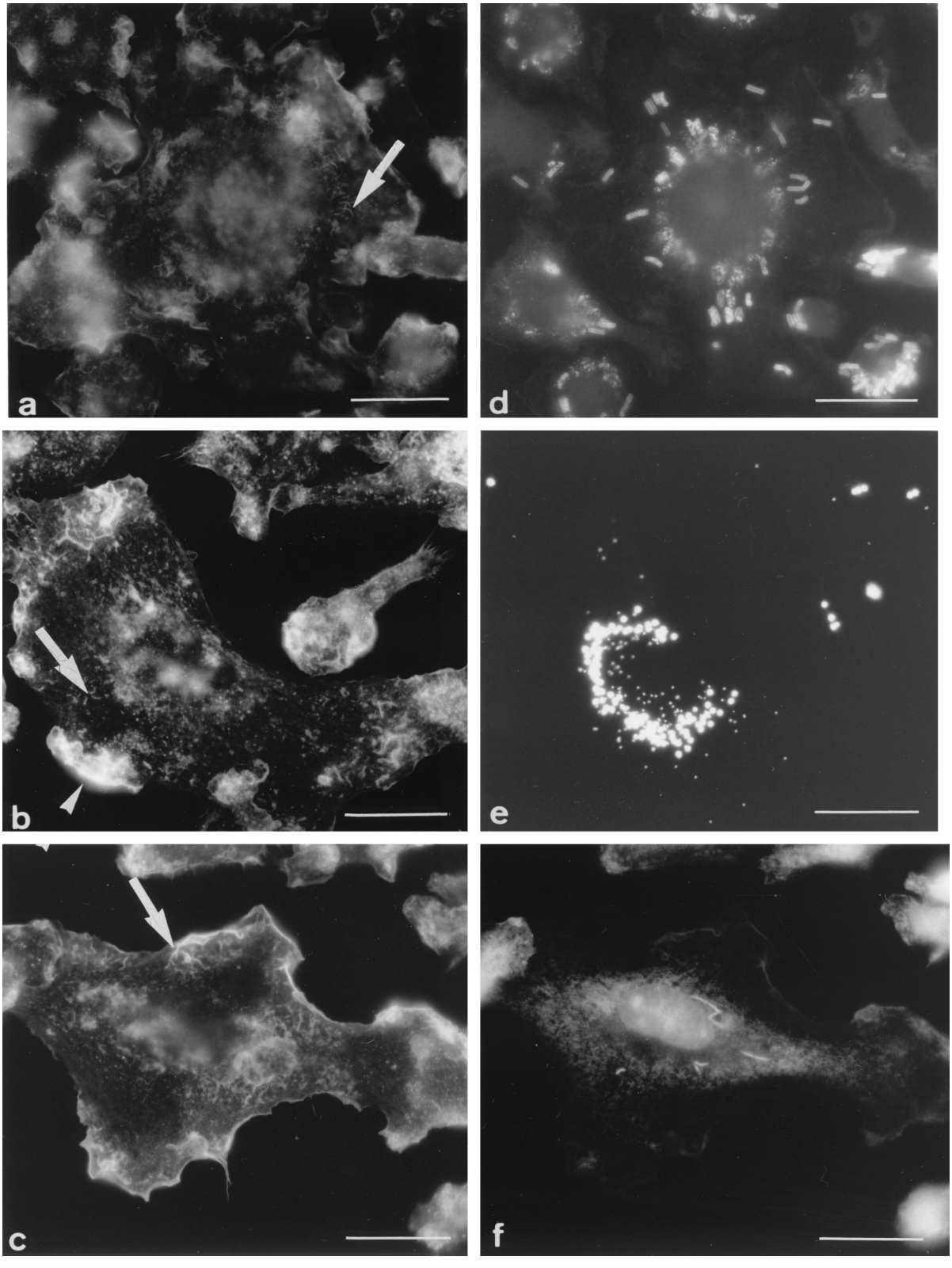

FIG. 3. Appearance of F-actin (a to c) and location of phagosomes (d to f) after phagocytic uptake of different particles. (a and d) *B. subtilis* with a 45-min chase after uptake; (b and e) fluoresbrite microspheres with a 2-h chase after uptake; (c and f) *M. smegmatis* 1 day after phagocytic uptake. In all cases, the F-actin network retained the appearance and distribution pattern observed in uninfected cells, i.e., small filaments (arrows) and zero, one, or two patches (arrowheads). At these time points, phagosomes were gathered around the nucleus in all cases. Bars = 5 μm.

dure gave, however, identical results. After the 4-h infection period (day 0), the morphological appearance and distribution pattern of F-actin remained unchanged with respect to those of F-actin in uninfected cells cultured in parallel (Fig. 2a). The network of small filaments was observed in all the cells (Table 1). As was the case for uninfected Mϕs, 25% of the cells displayed no patches while 75% showed one or two (Table 1). Interestingly, infection of cells with higher bacterial loads had no effect on the morphological appearance of F-actin (not shown). Afterward, dramatic changes in the distribution and appearance of F-actin were observed. At day 1 postinfection, F-actin gathered into large patches located at the cell periphery (Fig. 2b) in about 80% of the cells (Table 1); filaments were still observed, although in reduced amounts, and they were smaller. Starting from day 2, and increasingly so with time after infection, the short filaments completely disappeared. Cells displayed instead a myriad of tiny punctate structures that were scattered throughout the cells (Fig. 2c). The large patches fragmented into smaller ones (Fig. 2c) or even completely disappeared (as in Fig. 1d). These results show that virulent *M. avium* causes a dramatic alteration of the host cell's actin filament network with a clear shift from categories 1 and 2 to category 3 at day 1 and to category 4 within the following days postinfection.

To rule out the possibility that fragmentation of the actin filaments was only a consequence of phagocytosis and/or of the presence of phagosomes within Mϕs, the same studies were carried out after phagocytic uptake of (i) the nonpathogenic and rapidly degraded bacterium *B. subtilis* or (ii) fluorescent hydrophobic latex beads (fluoresbrite microspheres). An additional advantage of using these two particles is that it gave us the possibility of determining whether a relationship between fragmentation of the actin filaments and phagosome maturation could be established. Indeed, *B. subtilis*-containing phagosomes mature normally and fuse with lysosomes within less than 15 min after uptake (11, 28), whereas phagosomes containing hydrophobic latex beads remain immature and early endosome-like for at least 3 h (7, 11) (versus indefinitely for phagosomes containing pathogenic mycobacteria). After phagocytic uptake of *B. subtilis* (Fig. 3a) or fluoresbrite microspheres (Fig. 3b), the F-actin network retained the morphological appearance and distribution pattern observed within uninfected cells. The short and thin filaments were observed in all cells, with 25% of the cells displaying no patches and 75% showing one or two (Table 1). In some cells, some of the small filaments seemed to have a punctate appearance. By scanning through the thickness of the cell, however, it was clear that these dots always corresponded to small filaments. These results indicate that fragmentation of the F-actin network is not caused merely by phagocytic uptake and/or the presence of phagosomes.

To determine whether F-actin fragmentation was specific to pathogenic mycobacteria, Mϕs were processed for visualization of F-actin immediately and 1 or 2 days after phagocytosis of *M. smegmatis*. This strain is a nonpathogenic, rapidly growing mycobacterium when cultured in nutrient broth, and it is unable to survive within Mϕs (32). As before with *B. subtilis* or latex beads, the morphological appearance and distribution of F-actin were identical to those observed in uninfected cells (Fig. 3c), with 25% of the cells showing no patches and 75% displaying one or two (Table 1). Even at 2 days postinfection, there were no signs of clustering into patches or fragmentation of the filaments into tiny punctate structures (data not shown).

Alteration of the F-actin network delays movement of *M. avium*-containing phagosomes towards the juxtanuclear region. The distribution of phagosomes was examined at selected intervals after phagocytic uptake of the different particles, in the same cells as those stained for F-actin. Immediately after phagocytic uptake, phagosomes were scattered within the cells in all cases, as expected. Shortly afterward, i.e., 45 min for *B. subtilis* and 2 h for latex particles, phagosomes containing either *B. subtilis* (Fig. 3d) or hydrophobic latex beads (Fig. 3e) gathered around the nucleus in 95% of the cells (Table 2), thereby indicating that early-endosome-like phagosomes, like phagolysosomes, move towards the juxtanuclear region. In contrast, phagosomes with the virulent *M. avium* strain were still scattered at 2 and 24 h postinfection (Fig. 2d and e; Table 2), which was not the case for *M. smegmatis*-containing phagosomes (Table 2). By day 6, phagosomes had, however, gathered around the nucleus (Fig. 2f; Table 2). These results suggest that the F-actin network is involved in the movement of phagosomes towards the juxtanuclear region.

TABLE 2. Percentages of cells displaying scattered phagosomes or phagosomes gathered around the nucleus at selected time points after phagocytic uptake of particles[a]

Phagocytic particle	Time after uptake	% Cells displaying[b]:	
		S	N
B. subtilis	10 min	95	5
	45 min	4	96
	2 h	1	99
Latex beads	30 min	77	23
	2 h	5	95
M. smegmatis	1 day	28	72
M. avium	2 h	98	2
	1 day	77	23
	2 days	33	67
	6 days	4	96

[a] Counts were made on the same cells as for Table 1. In all cases, the standard error of the mean was less than 10%.
[b] S, scattered phagosomes; N, phagosomes gathered around the nucleus.

Does F-actin colocalize with early-endosome-like phagosomes or phagolysosomes? The distribution of phagosomes with respect to the F-actin network was then examined for cells subjected to phagocytosis of either *B. subtilis* or *M. avium* with the aim of determining whether immature early-endosome-like phagosomes (containing *B. subtilis* and less than 15 min old or containing *M. avium*) or phagolysosomes (containing *B. subtilis* and more than 15 min old) colocalized, or could be observed in close association, with F-actin.

As shown before for many other particles (reviewed in references 22, 23, and 35), F-actin assembled into patches at the region of the plasma membrane that contacts the particle during phagocytic uptake of *B. subtilis* and surrounded bacteria during their internalization (Fig. 4a and c). This seems to be a rapid and transient event, as very few bacteria were capped with F-actin in a given cell after 5 min of phagocytosis. For *M. avium*, such caps of F-actin were observed only when bacteria were engulfed in clumps (data not shown), which is a rare event in our experimental conditions. The fact that F-actin was not observed during the engulfment process of single bacteria could be explained by the small size of bacteria and/or a limited recruitment of F-actin to their site of internalization.

Phalloidin-stained F-actin was not observed in close proximity to newly formed *B. subtilis*- or *M. avium*-containing phagosomes. We then examined whether the immature early-endosome-like phagosomes containing *M. avium* were associated with F-actin at any given time postinfection. Interestingly,

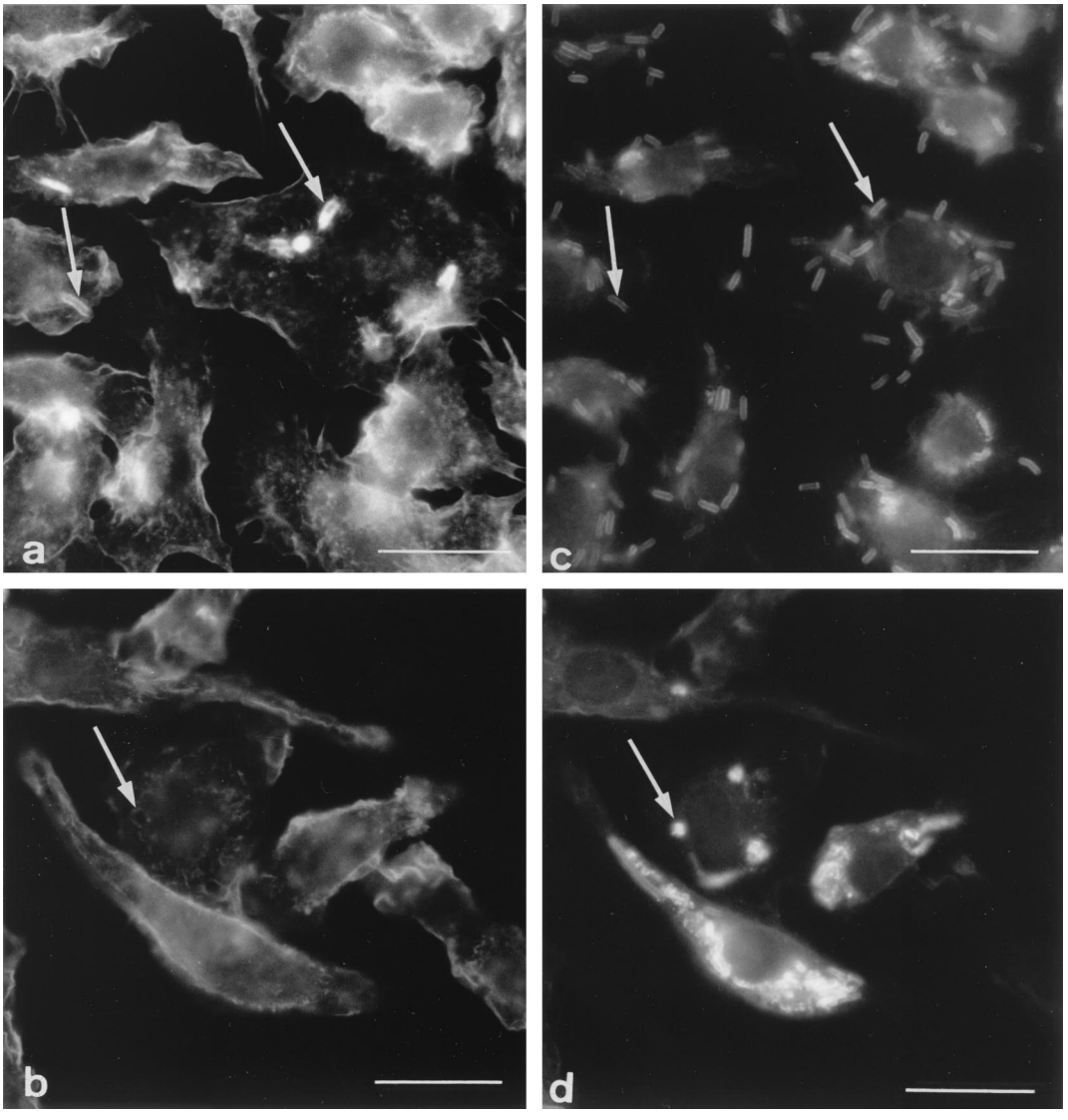

FIG. 4. Colocalization of F-actin and phagosomes. (a and c) Five-minute exposure to *B. subtilis* showing the typical cap of F-actin (a; arrows) around bacteria during phagocytic uptake (c; arrows); (b and d) 45-min exposure of cells to *B. subtilis* showing a ring of F-actin (b; arrow) around a phagolysosome (d; arrow). Bars = 5 μm.

the labeling with the monoclonal antibody raised against the mycobacterial cell wall glycopeptidolipids was mostly restricted to the phagosomes throughout the 10-day period of observation. This greatly facilitated the examination of the distribution of phagosomes in the cell with respect to actin. By conventional immunofluorescence microscopy as well as by confocal microscopy, we observed no association whatsoever of F-actin with the *M. avium*-containing phagosomes between 0 and 10 days postinfection. In particular, phagosomes were never found within, or in the vicinity of, the large patches of F-actin observed in the cortical region at day 1.

Because actin filaments have been shown to facilitate fusion events at late stages of the endocytic pathway (16, 39), *B. subtilis*-containing phagolysosomes were also examined for possible association with F-actin. Such phagolysosomes can be differentiated from immature and maturing phagosomes by the morphological appearance of immunolabeled bacteria, which are rod shaped in the immature and maturing phagosomes and then become rounded as bacteria undergo degradation within phagolysosomes (28). For most phagolysosomes, no clear association with actin was observed. In rare instances, however, a ring of F-actin around phagolysosomes was observed (compare Fig. 4b and d). This suggests that F-actin can associate with phagolysosomes; this phenomenon appears to be transient, and it is probably followed by rapid disassembly.

To conclude, our data clearly indicate that pathogenic *M. avium*, as opposed to other particles including nonpathogenic mycobacteria, disrupt the actin filament network in BMD mouse Mϕs. The observed 1-day lag suggests that bacteria need to first synthesize new components and/or reorganize their wall constituents within the phagosomal environment before being able to disrupt the actin filament network. This event is not the cause for inhibition of phagosome maturation since other particles (hydrophobic latex beads) can prevent phagosome maturation without altering the actin filament network. However, it could be one of the reasons for the delayed and limited intermingling of contents between early endosomes and immature *M. avium*-containing phagosomes since the lag in acquisition of HRP by *M. avium*-containing phagosomes seems to coincide with the disorganization of the actin filament network (11). Disruption of the actin cytoskeleton by pathogenic mycobacteria could also serve as a strategy to coun-

teract other microbicidal activities of Mϕs such as the production of toxic nitrogen derivatives that play an important role in killing endoparasites (30). It has indeed been shown that disruption of the actin filaments prevents the nitric oxide synthase induction process and inhibits its enzymatic activity in activated Mϕs (17). The mechanism by which pathogenic mycobacteria induce disruption of the actin filament network and the bacterial and cell components implicated in this process are currently under investigation.

ACKNOWLEDGMENTS

We thank Patrick Brennan and John T. Belisle (Colorado State University, Fort Collins, Colo.) for kindly providing us with the monoclonal antibody CS-17. We also thank P. Pillot (Pasteur Institute, Paris, France) for the generous gift of anti-*B. subtilis* antibodies, Georg Plum (Institute für Medizinische, Mikrobiologie und Hygiene, Cologne, Germany) for providing the strain of *M. smegmatis*, and Patrick Stragier (Institut de Chimie et Biophysique, Paris, France) for the strain of *B. subtilis*. We are especially grateful to Patrick Berche (INSERM U411, UFR de Médecine Necker, Paris, France) for support and helpful advice.

This work received financial support from the Institut National de la Santé et de La Recherche Médicale (funds to INSERM Unit 411). Isabelle Guérin received a scholarship from the Ministère de la Recherche et de la Technologie. Monoclonal antibody CS-17 was produced with funds from the National Institute of Allergy and Infectious Diseases, National Institutes of Health, contract NO1-AI-25147, entitled Tuberculosis Research Materials.

REFERENCES

1. **Alvarez-Dominguez, C., L. Mayorga, and P. D. Stahl.** 1999. Sequential maturation of phagosomes provides unique targets for pathogens, p. 285–297. *In* S. Gordon (ed.), Advances in cell and molecular biology of membranes and organelles, vol. 5. JAI Press Inc., Stamford, Conn.
2. **Armstrong, J. A., and P. d'Arcy Hart.** 1971. Response of cultured macrophages to *Mycobacterium tuberculosis*, with observations on fusion of lysosomes with phagosomes. J. Exp. Med. **134:**713–740.
3. **Beron, W., C. Alvarez-Dominguez, L. Mayorga, and P. D. Stahl.** 1995. Membrane trafficking along the phagocytic pathway. Trends Cell Biol. **5:**100–104.
4. **Blocker, A., F. F. Severin, A. Habermann, A. A. Hyman, G. Griffiths, and J. K. Burkhardt.** 1996. Microtubule-associated protein dependent binding of phagosomes to microtubules. J. Biol. Chem. **271:**3803–3811.
5. **Blocker, A., G. Griffiths, J.-C. Olivo, A. A. Hyman, and F. F. Severin.** 1998. A role for microtubule dynamics in phagosome movement. J. Cell. Sci. **111:**303–312.
6. **Clemens, D. L., and M. A. Horwitz.** 1996. The *Mycobacterium tuberculosis* phagosome interacts with early endosomes and is accessible to exogenously administered transferrin. J. Exp. Med. **184:**1349–1355.
7. **de Chastellier, C., and L. Thilo.** 1997. Phagosome maturation and fusion with lysosomes in relation to surface property and size of the phagocytic particle. Eur. J. Cell Biol. **74:**49–62.
8. **de Chastellier, C., and L. Thilo.** 1999. Mycobacteria and the endocytic pathway, p. 107–135. *In* S. Gordon (ed.), Advances in cell and molecular biology of membranes and organelles, vol. 6. JAI Press Inc., Stamford, Conn.
9. **de Chastellier, C., T. Lang, A. Ryter, and L. Thilo.** 1987. Exchange kinetics and composition of endocytic membranes in terms of plasma membrane constituents: a morphometric study in macrophages. Eur. J. Cell Biol. **44:** 112–123.
10. **de Chastellier, C., C. Fréhel, C. Offredo, and E. Skamene.** 1993. Implication of phagosome-lysosome fusion in restriction of *Mycobacterium avium* growth in bone marrow macrophages from genetically resistant mice. Infect. Immun. **61:**3775–3784.
11. **de Chastellier, C., T. Lang, and L. Thilo.** 1995. Phagocytic processing of the macrophage endoparasite, *Mycobacterium avium*, in comparison to phagosomes which contain *Bacillus subtilis* or latex beads. Eur. J. Cell Biol. **68:** 167–182.
12. **Desjardins, M.** 1995. Biogenesis of phagolysosomes: the 'kiss and run' hypothesis. Trends Cell Biol. **5:**183–186.
13. **Desjardins, M., J. E. Celis, G. van Meer, H. Dieplinger, A. Jahraus, G. Griffiths, and L. A. Huber.** 1994. Molecular characterization of phagosomes. J. Biol. Chem. **269:**32194–32200.
14. **Desjardins, M., L. A. Huber, R. G. Parton, and G. Griffiths.** 1994. Biogenesis of phagolysosomes proceeds through a sequential series of interactions with the endocytic apparatus. J. Cell Biol. **124:**677–688.
15. **Dramsi, S., and P. Cossart.** 1998. Intracellular pathogens and the actin cytoskeleton. Annu. Rev. Cell Dev. Biol. **14:**137–166.
16. **Durrbach, A., D. Louvard, and E. Coudrier.** 1996. Actin filaments facilitate two steps of endocytosis. J. Cell. Sci. **109:**457–465.
17. **Fernandes, P. D., H. M. Araujo, V. Riveros-Moreno, and J. Assreuy.** 1996. Depolymerization of macrophage microfilaments prevents induction and inhibits activity of nitric oxide synthase. Eur. J. Cell Biol. **71:**356–362.
18. **Fréhel, C., C. de Chastellier, T. Lang, and N. Rastogi.** 1986. Evidence for inhibition of fusion of lysosomal and prelysosomal compartments with phagosomes in macrophages infected with pathogenic *Mycobacterium avium*. Infect. Immun. **52:**252–262.
19. **Fréhel, C., C. de Chastellier, C. Offredo, and P. Berche.** 1991. Intramacrophage growth of *Mycobacterium avium* during infection of mice. Infect. Immun. **59:**2207–2214.
20. **Fréhel, C., C. Offredo, and C. de Chastellier.** 1997. The phagosomal environment protects virulent *Mycobacterium avium* from killing and destruction by clarithromycin. Infect. Immun. **65:**2792–2802.
21. **Gottlieb, T. A., I. E. Ivanov, M. Adesnik, and D. D. Sabatini.** 1993. Actin microfilaments play a critical role in endocytosis at the apical but not the basolateral surface of polarized epithelial cells. J. Cell Biol. **120:**695–710.
22. **Greenberg, S.** 1995. Signal transduction of phagocytosis. Trends Cell Biol. **5:**93–99.
23. **Greenberg, S., and S. C. Silverstein.** 1993. Phagocytosis, p. 941–964. *In* W. E. Paul (ed.), Fundamental immunology, 3rd ed. Raven Press Ltd., New York, N.Y.
24. **Greenberg, S., K. Burridge, and S. C. Silverstein.** 1990. Colocalization of F-actin and talin during Fc receptor-mediated phagocytosis in mouse macrophages. J. Exp. Med. **172:**1853–1856.
25. **Higley, S., and M. Way.** 1997. Actin and cell pathogenesis. Curr. Opin. Cell Biol. **9:**62–69.
26. **Jackman, M. R., W. Shurety, J. A. Ellis, and J. P. Luzio.** 1994. Inhibition of apical but not basolateral endocytosis of ricin and folate in Caco-2 cells by cytochalasin D. J. Cell Sci. **107:**2547–2556.
27. **Kübler, E., and H. Riezman.** 1993. Actin and fimbrin are required for the internalization step of endocytosis in yeast. EMBO J. **12:**2855–2862.
28. **Lang, T., C. de Chastellier, A. Ryter, and L. Thilo.** 1988. Endocytic membrane traffic with respect to phagosomes in macrophages infected with nonpathogenic bacteria: phagosomal membrane acquires the same composition as lysosomal membrane. Eur. J. Cell Biol. **46:**39–50.
29. **Murphy, C., R. Saffrich, M. Grummt, H. Gournier, V. Rybin, M. Rubino, P. Auvinen, A. Lütcke, R. G. Parton, and M. Zerial.** 1996. Endosome dynamics regulated by a Rho protein. Nature **384:**427–432.
30. **Nathan, C. F., and J. B. Hibbs.** 1991. Role of nitric oxide synthesis in macrophage antimicrobial activity. Curr. Opin. Immunol. **3:**65–70.
31. **Pedrosa, J., M. Florido, Z. M. Kunze, A. G. Castro, F. Portaels, J. McFadden, M. T. Silva, and R. Appelberg.** 1994. Characterization of the virulence of *Mycobacterium avium* complex (MAC) isolates in mice. Clin. Exp. Immunol. **98:**210–216.
32. **Plum, G., M. Brenden, J. E. Clark-Curtiss, and G. Pulverer.** 1997. Cloning, sequencing and expression of the *mig* gene of *Mycobacterium avium*, which codes for a secreted macrophage-induced protein. Infect. Immun. **65:**4548–4557.
33. **Riezman, H., A. Munn, M. I. Geli, and L. Hicke.** 1996. Actin-, myosin- and ubiquitin-dependent endocytosis. Experientia **52:**1033–1041.
34. **Russell, D. G., J. Dant, and S. Sturgill-Koszycki.** 1996. *Mycobacterium avium*- and *Mycobacterium tuberculosis*-containing vacuoles are dynamic, fusion-competent vesicles that are accessible to glycospingolipids from the host cell plasmalemma. J. Immunol. **156:**4764–4773.
35. **Silverstein, S. C., S. Greenberg, F. di Virgilio, and T. Steinberg.** 1989. Phagocytosis, p. 703–720. *In* W. E. Paul (ed.), Fundamental immunology. Raven Press Ltd., New York, N.Y.
36. **Steinman, R. M., S. E. Brodie, and Z. A. Cohn.** 1976. Membrane flow during endocytosis. A stereological analysis. J. Cell Biol. **68:**665–687.
37. **Sturgill-Koszycki, S., N. E. Schaible, and D. G. Russell.** 1996. *Mycobacterium*-containing phagosomes are accessible to early endosomes and reflect a transitional state in normal phagosome biogenesis. EMBO J. **15:**6960–6968.
38. **Swanson, J. A., A. Locke, P. Ansel, and P. J. Hollenbeck.** 1992. Radial movement of lysosomes along microtubules in permeabilized macrophages. J. Cell Sci. **103:**201–209.
39. **van Deurs, B., P. K. Holm, L. Kayser, and K. Sandvig.** 1995. Delivery to lysosomes in the human carcinoma cell line Hep-2 involves an actin filament-facilitated fusion between mature endosomes and preexisting lysosomes. Eur. J. Cell Biol. **66:**309–323.
40. **Ward, D. M., R. Ajioka, and J. Kaplan.** 1989. Cohort movement of different ligands and receptors in the intracellular endocytic pathway of alveolar macrophages. J. Biol. Chem. **264:**8164–8170.

Editor: J. T. Barbieri